

# Crystallite shape, dielectric constant and functional data analysis of various cotton fibres using WAXS data

V V Manju<sup>1</sup>, S Divakara<sup>1</sup>, Divakaran Karthik<sup>2</sup> & R Somashekar<sup>2,3,a</sup>

<sup>1</sup>Vidyavardhaka College of Engineering, Visvesvaraya Technological University, Gokulam, 3<sup>rd</sup> Stage, Mysuru 570 002, India

<sup>2</sup>Center for Material science, University of Mysore, Vijnana Bhavan, Mysuru 570 006, India

<sup>3</sup>Department of Physics, Regional College of Education, Mysuru 570 006, India

Received 19 July 2018; revised received and accepted 8 May 2019

Four different varieties of cotton fibres have been used for X-ray diffraction study using in-house programs. X-ray data have been corrected for instrumental broadening and Lorentz polarization factors before using them for further analysis. Using Peakfit® program, 13-15 Bragg reflections are identified and cell parameters are determined by CHECKCELL®. Full width at half maxima (FWHM) of these reflections are used to estimate the crystallite size and strain along [hkl] directions. Using these results and employing a novel method, a 3-dimensional image of the crystallite shapes in these cotton fibres are computed. Employing Lorenz-Mie theory of scattering of electromagnetic radiation by molecules embedded in dielectric spheres, the dielectric constant of cellulose along amorphous region has been computed. This technique can be extended to any material of interest. Correlation among varieties of fibres and each physical parameter like crystallite size, strain, tenacity and staple length have been investigated using functional analysis, which shows the correlation between physical parameters with varieties of cotton fibres.

**Keywords:** Cotton, Crystallite shape, Dielectric constant, Functional data analysis, Natural fibres, X-ray diffraction

## 1 Introduction

Cotton, one of the widely used natural fibres, plays an important role in the textile industry because of its cost effectiveness. Cotton is essentially pure cellulose and a polymer consisting of units of anhydro-glucopyranose linked through  $\beta$ -1-4 linkages with its empirical formula  $(C_6H_{10}O_5)_n$ ; the value of “n” being as high as 4000-5000 and molecular weight 8,00,00<sup>1-3</sup>. Historically, the structure property relation in cotton fibre is considered to be very important in textile industry<sup>4,5</sup>. Also, cotton fabrics provide desirable properties, like absorbency, breathability and softness<sup>6</sup>. Researchers around the globe are involved in making modification in the structure of cotton so as to attain more stability<sup>7</sup>. It is interesting to know that people are studying to make cotton conducting, repellent to oil & water, and fire retardant<sup>8-10</sup>. In this study, an attempt has been made to define structure property relations among these fibres using X-ray diffraction studies. For this, DCH-32, MCU-5, Shankar and LRA cotton samples are chosen based on their tenacity, staple lengths and origin. The quality of a cotton fibre can be judged on many factors, like

staple length, maturity, fineness, etc.<sup>11</sup>. The correlation among varieties of fibres and each physical parameters, like crystallite size, tenacity and staple length has been obtained using functional data analysis to arrive with the most probable dependencies.

## 2 Materials and Methods

### 2.1 Materials

DCH-32, MCU-5, LRA and Shankar varieties of cotton were used. DCH-32, cultivated<sup>12</sup> in parts of Karnataka, Tamilnadu and Madhya Pradesh of India, is an interspecific hybrid of DS 58 (*G.hirsutum*) and XS B 425 YF(*G.barbadense*). MCU-5 is a cross breed developed from Sea Island, 542, MCU 1, MCU 2 and Gatooma. LRA is a cross breed developed from Laxmi, Reba B.50 and AC 122. Shankar is also a cross breed derived from two varieties viz G. Dot 100 and G. Cot 100<sup>12-14</sup>. Table 1 gives the physical details of all the cotton fibres used for this study.

### 2.2 X-ray Diffraction Studies

The small bundles of samples were clamped into a sample holder, which was then mounted on the goniometer in such a way that the rotational axis becomes parallel to the fibre axis and perpendicular to

<sup>a</sup>Corresponding author.  
E-mail: rs@physics.uni-mysore.ac.in

the X-ray beam. Here, we have used an imaging plate system (DIP-3200) with dimensions  $440 \times 240 \text{ mm}^2$ , which was moved parallel to the axis of rotation. The wavelength of X-ray radiation was  $0.71073 \text{ \AA}$  (Mo target). The X-ray generator (RIGAKU) settings were 50 kV and 32 mA. The time of exposure was kept 400s. Equatorial scans of intensity versus  $2\theta$  were carried out using the MOSFLM software supplied with instrument. The X-ray diffraction pattern recorded for the different samples from the imaging plate system was converted into the line profile format and is shown in Fig. 1.

### 3 Results and Discussion

Using Peakfit<sup>®</sup>(ref.15), the obtained profile is simulated by Gaussian de-convolution method and 13-15 reflections are identified for each cotton fibre.

Table 1 — Various physical parameters (Standard) of cotton fibres under study

Cotton	Span length, mm	Tensile strength g/tex	Avg crystallite size, $\text{\AA}$ [Calculated]
DCH-32	$36 \pm 3$	$23.0 \pm 2$	51.51
MCU-5	$30 \pm 3$	$20.8 \pm 2$	46.76
Shankar	$29 \pm 3$	$22.2 \pm 2$	44.49
LRA	$28 \pm 3$	$19.8 \pm 2$	38.70

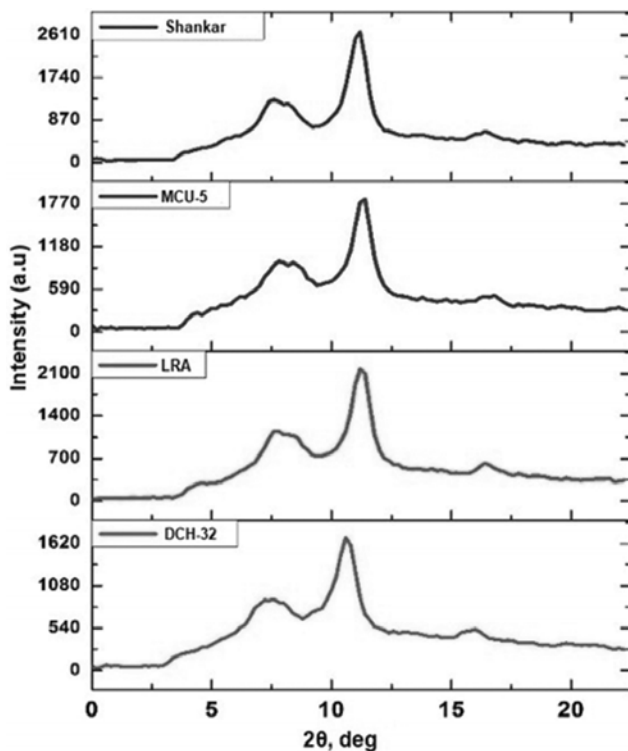


Fig. 1 — X-ray diffraction patterns of cotton fibres

These Bragg reflections are further used along with a program Checkcell<sup>®</sup> to compute cell parameters and identify (hkl) directions. The observed reflections are indexed to a monoclinic unit cell with dimensions  $a = 7.350 \text{ \AA}$ ,  $b = 8.220 \text{ \AA}$ ,  $c = 10.370 \text{ \AA}$  and  $\gamma = 96.28^\circ$  (ref. 16). Peakfit<sup>®</sup> program also gives full width at half maxima for each one of these Bragg reflections using Scherrer equation, we have estimated the crystallite size and strain in these samples, shown below:

$$D_s = \frac{K\lambda}{\beta \cos \theta} \quad \dots (1)$$

where  $D_s$  is the crystallite size in  $\text{\AA}$ ;  $K$ , the dimensionless shape factor which we have taken to be 0.9;  $\lambda$ , wavelength in  $\text{\AA}$ ;  $\beta$ , the line broadening at half the intensity measured in radians; and  $\theta$ , the Bragg angle. Lattice strain was determined using the following equation:

$$\frac{\delta d}{d} = \frac{\beta}{\tan \theta} \quad \dots (2)$$

where  $\frac{\delta d}{d}$  is the lattice strain;  $\beta$ , the line broadening at half the maximum intensity (FWHM); and  $\theta$ , the Bragg angle in degree.

#### 3.1 Procedure for Obtaining 3-dimensional Image of Crystallite Shapes

Using simple spherical coordinates properties, and employing cell parameters and crystallite size, we have determined the spherical angles  $\theta$  and  $\phi$  for the observed [hkl] directions. For this purpose, a program (FORTRAN<sup>®</sup>) has been used to evaluate the spherical coordinate representation for a given set of [hkl] and size values. Now, there are three variables, namely  $\theta$ ,  $\phi$  and crystallite size for all considered reflections. These points were plotted as surface plot along with special commands in order to get the desired view of 3-dimensional surface plot using Gnuplot<sup>®</sup>(ref. 17). The X-ray image surface is the envelop on the tip of the crystallite size vectors, along different Bragg directions. In this plot, the negative values of crystallite size is also included to visualize holistic shape of the crystallite region. The origin inside Fig. 2 represents the point at which X-ray beam hits the sample. From this origin, we have drawn a few Bragg reflection directions in order to represent them as a 3-dimensional entity. The lengths of the vectors do not represent the magnitude of size along that direction. These obtained shapes, illustrate

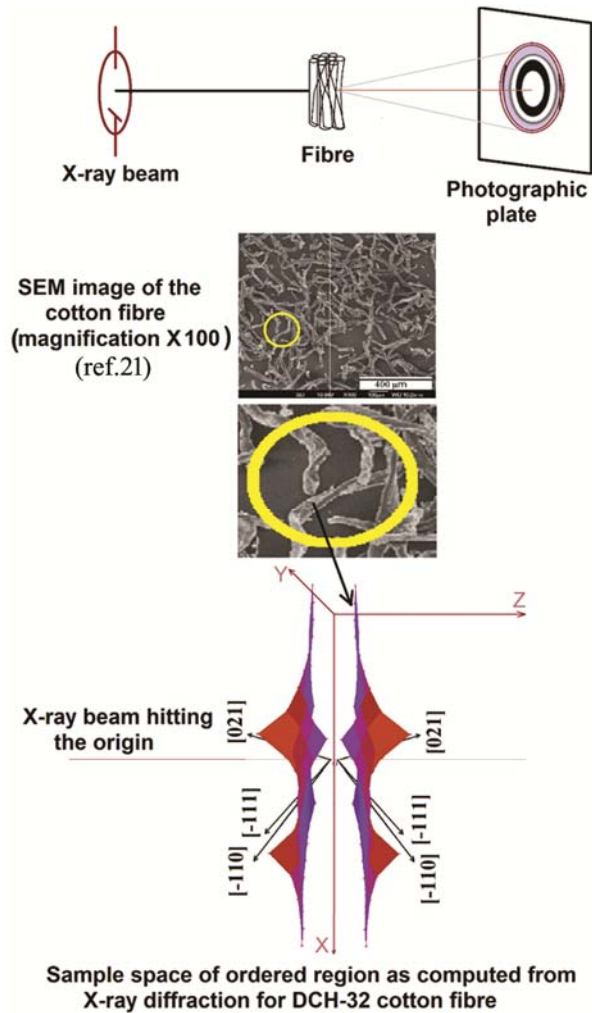


Fig. 2 — Schematic representation of crystallite ordered region calculated from XRD

that the computed X-ray image of crystallite shape is not an ellipsoid; as assumed earlier by some researchers (ref.18) in order to develop mathematical models to understand the X-ray diffraction patterns from a sample. The computed X-ray image of DCH-32, MCU-5, Shankar and LRA cotton fibres respectively are shown in Figs 3 and 4. Figure 2 shows the X-ray beam hitting the sample and the obtained images captured on the photographic plate.

### 3.2 Functional Data Analysis

Using functional data analysis<sup>19</sup>, we have computed probable variation in a physical parameter with respect to an independent variable of consideration. For completeness, different equations have been used. The functional data analysis for cotton fibres has been carried out by using physical parameters (crystallite

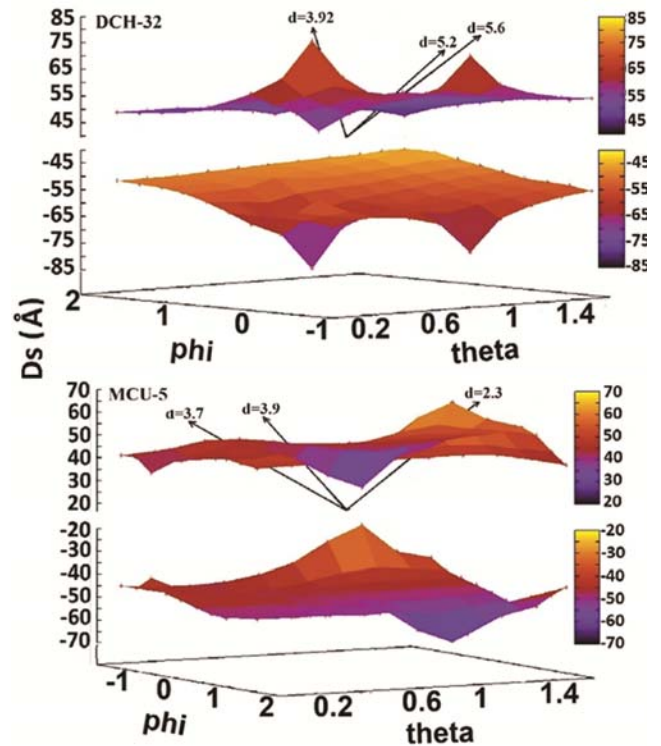


Fig. 3 — Computed X-ray image of DCH-32 and MCU-5 cotton fibres.

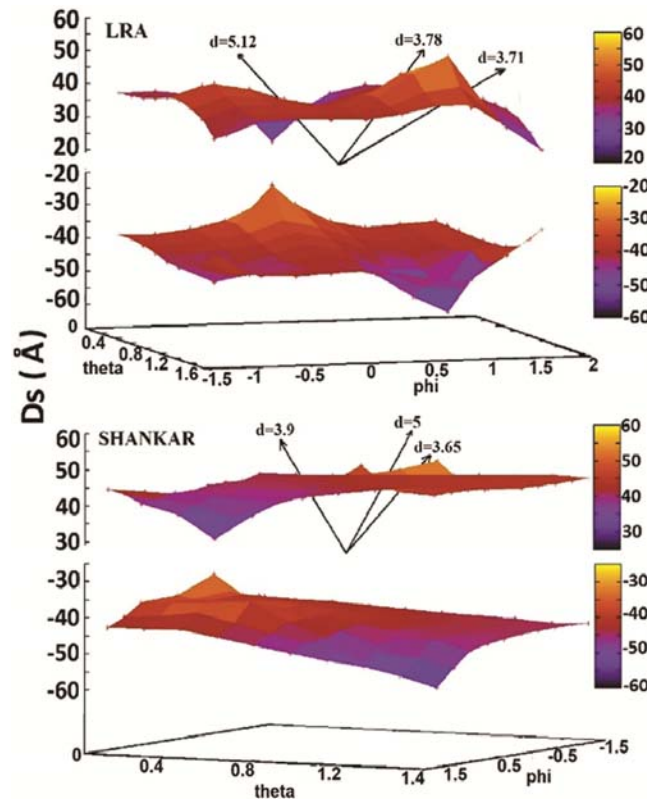


Fig. 4 — Computed X-ray image of LRA and Shankar cotton fibres.

size, tenacity and span length) of interest as  $\theta$ , and the variable of measurement ( $t$ ) as variety of cotton fibres (1,2,3,4 represents DCH-32, MCU-5, Shankar and LRA cotton fibres respectively in Figs 5 and 6). Six measurements of physical parameters have been made. Tenacity and span length have also been considered for analysis as mentioned in Table 1. Let

the value of  $\theta$  observed for a  $j^{\text{th}}$  sample on the  $i^{\text{th}}$  trial be represented as:

$$\begin{aligned} \theta_{ij} &= \theta_i(t_j) + \epsilon_{ij} = \mu(t_{ij}) + \sum_{k=1}^{\infty} \xi_{ik} \Phi_k(t_{ij}) + \epsilon_{ij} \\ &\approx \mu(t_{ij}) + \sum_{k=1}^M \xi_{ik} \Phi_k(t_{ij}) + \epsilon_{ij} \quad \dots (3) \end{aligned}$$

where  $\epsilon_{ij}$  are the random experimental errors. The

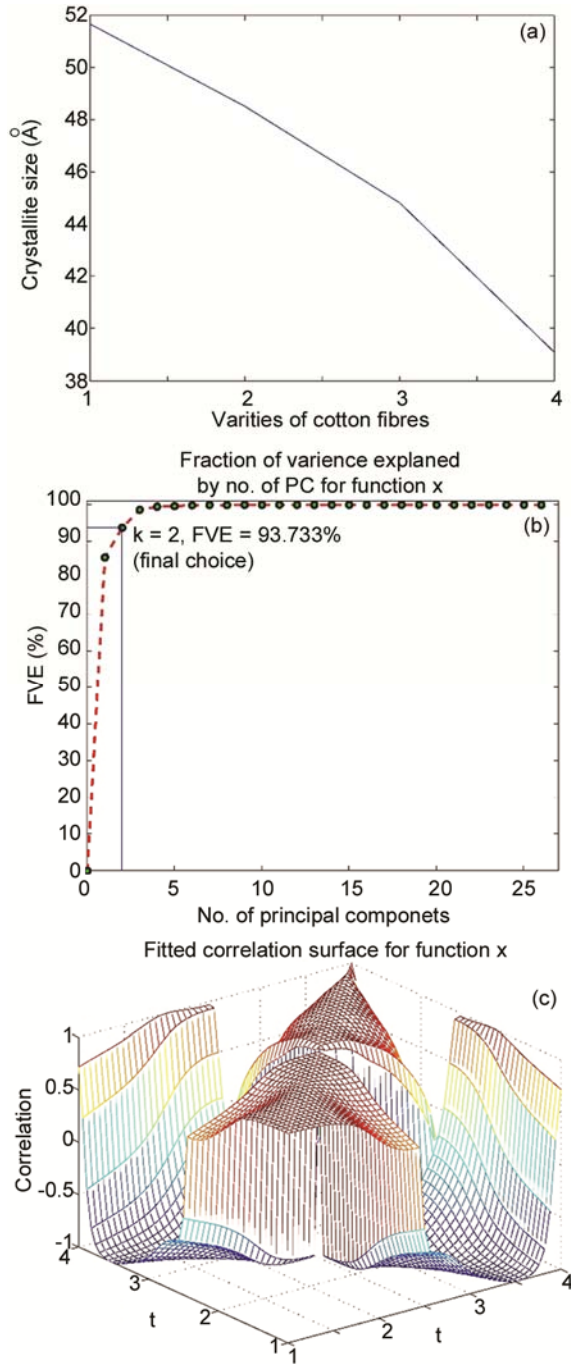


Fig. 5 — Functional data analysis results obtained as a function of crystallite size, (a) mean variation (b) variation principal components and (c) correlation surface

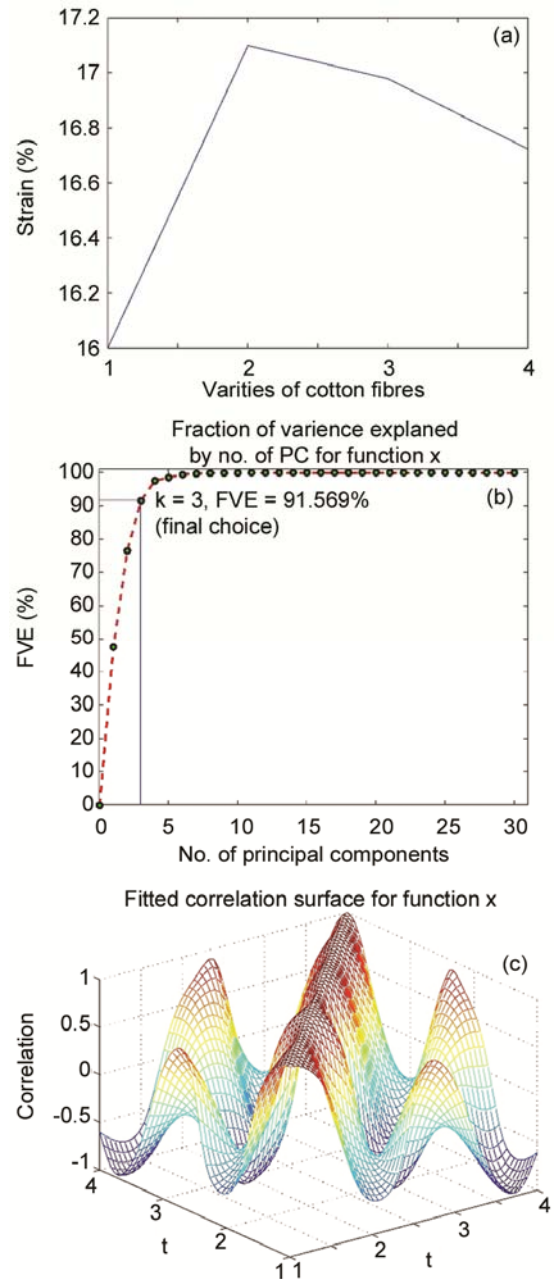


Fig. 6 — Functional data analysis results obtained as a function of lattice strain, (a) mean variation (b) variation principal components and (c) correlation surface

Table 2 — Microstructure parameters of DCH-32 cotton fibre

2 $\theta$ , deg	hkl	d, Å	Ds, Å	g, %	q	q <sup>3</sup>
3.94	001	10.61	64.35	29.68	0.65	0.27
5.56	100	7.52	57.94	23.36	0.58	0.20
6.33	011	6.60	54.29	21.90	0.55	0.16
7.15	101	5.85	56.59	18.60	0.57	0.19
7.45	-110	5.61	50.26	20.10	0.51	0.13
8.15	-111	5.13	74.68	12.37	0.75	0.43
9.17	-102	4.56	77.02	10.66	0.78	0.47
10.13	102	4.13	45.2	16.43	0.45	0.09
10.67	021	3.92	98.38	7.17	1	1
11.42	-201	3.66	36.77	17.94	0.37	0.05
13.62	103	3.07	34.26	16.16	0.34	0.04
15.75	221	2.66	45.30	10.57	0.46	0.09
16.75	300	2.50	28.14	16.01	0.28	0.02
17.77	-302	2.36	43.49	9.77	0.44	0.08
19.51	-303	2.15	30.83	12.56	0.31	0.03
20.95	214	2.00	26.55	13.59	0.26	0.01

Ds—Crystallite size, g—Crystallite strain, q—Ds/Ds(max), q<sup>3</sup>cal=0.22 from equation, and standard deviation =0.061.

Table 3 — Microstructure parameters of MCU-5 cotton fibre

2 $\theta$ , deg	hkl	d, Å	Ds, Å	G, %	q	q <sup>3</sup>
5.55	100	7.54	38.44	35.29	0.30	0.02
7.9	002	5.30	32.79	29.07	0.26	0.01
8.73	111	4.79	35.93	24.01	0.28	0.02
10.74	021	3.90	37.04	18.94	0.29	0.02
11.31	112	3.70	126.00	5.29	1	1
11.44	-120	3.66	32.05	20.56	0.25	0.01
13.5	-113	3.10	39.87	14.01	0.31	0.03
15.2	212	2.76	36.48	13.61	0.28	0.02
16.72	300	2.51	57.07	7.91	0.45	0.09
18.08	114	2.32	62.67	6.67	0.49	0.12
18.88	-231	2.22	55.44	7.22	0.44	0.08
19.86	-232	2.12	55.96	6.80	0.44	0.08
21.79	-304	1.93	36.46	9.53	0.28	0.02
21.9	-323	1.92	8.48	40.77	0.06	0.00

Ds—Crystallite size, g—Crystallite strain, q—Ds/Ds(max), q<sup>3</sup>cal=0.11 from equation, and standard deviation =0.066

Table 4 — Microstructure parameters of Shankar cotton fibre

2 $\theta$ , deg	hkl	d, Å	Ds, Å	G, %	q	q <sup>3</sup>
7.46	-110	5.61	38.53	26.20	0.34	0.04
8.21	-111	5.10	30.14	30.44	0.26	0.01
10.72	021	3.91	41.02	17.14	0.36	0.04
11.15	200	3.76	112.18	6.02	1	1
11.47	-201	3.65	43.67	15.05	0.38	0.05
13.09	-202	3.20	39.53	14.57	0.35	0.04
14.67	113	2.86	31.08	16.55	0.27	0.02
16.46	-222	2.55	57.75	7.94	0.51	0.13
17.26	203	2.43	28.60	15.30	0.25	0.01
18.56	-312	2.26	45.10	9.03	0.40	0.06
19.95	223	2.11	65.86	5.76	0.58	0.20
21.54	042	1.95	33.43	10.51	0.29	0.02
23.18	331	1.82	11.56	28.27	0.10	0.00

Ds—Crystallite size, g—Crystallite strain, q—Ds/Ds(max), q<sup>3</sup>cal=0.13 from equation, and standard deviation =0.071

mean function for the parameter is then estimated by solving the optimization problem, as shown below:

$$\hat{\mu}(t) : \operatorname{argmin}_{f \in F} \sum_{i=1}^n \sum_{j=1}^{n_i} [\theta_{ij} - f(t_{ij})]^2 + \lambda \int_{\mathbb{R}_{\geq 0}} [f''(t)]^2 dt \dots (4)$$

where F is the class of square integrable function with at least two derivatives. Program Functional principal component analysis (FPCA)<sup>19</sup> is used for this purpose. The correlation between various parameters are given in Figs 5 and 6, which implies the correlation of

Table 5 — Microstructure parameters of LRA cotton fibre

2θ, deg	hkl	d, Å	Ds, Å	G, %	q	q <sup>3</sup>
7.11	101	5.88	22.44	47.20	0.22	0.01
8.16	-111	5.13	37.16	24.84	0.36	0.04
11.06	200	3.79	32.03	21.28	0.31	0.03
11.26	112	3.72	102.16	6.55	1	1
13.1	211	3.20	29.35	19.61	0.28	0.02
15.13	-221	2.77	32.57	15.31	0.31	0.03
16.37	-222	2.56	73.77	6.25	0.72	0.37
17.39	-222	2.41	37.29	11.65	0.36	0.04
18.8	-231	2.23	36.65	10.97	0.35	0.04
20.16	-313	2.08	31.68	11.84	0.31	0.02
21.48	042	1.96	36.79	9.58	0.36	0.04
22.89	-402	1.84	31.56	10.48	0.30	0.02
26.25	052	1.61	15.62	18.51	0.15	0.00
30.95	161	1.37	22.85	10.76	0.22	0.01

Ds –Crystallite size, q –Crystallite strain, q –Ds/Ds(max), q<sup>3</sup>cal=0.12 from equation, and standard deviation =0.069

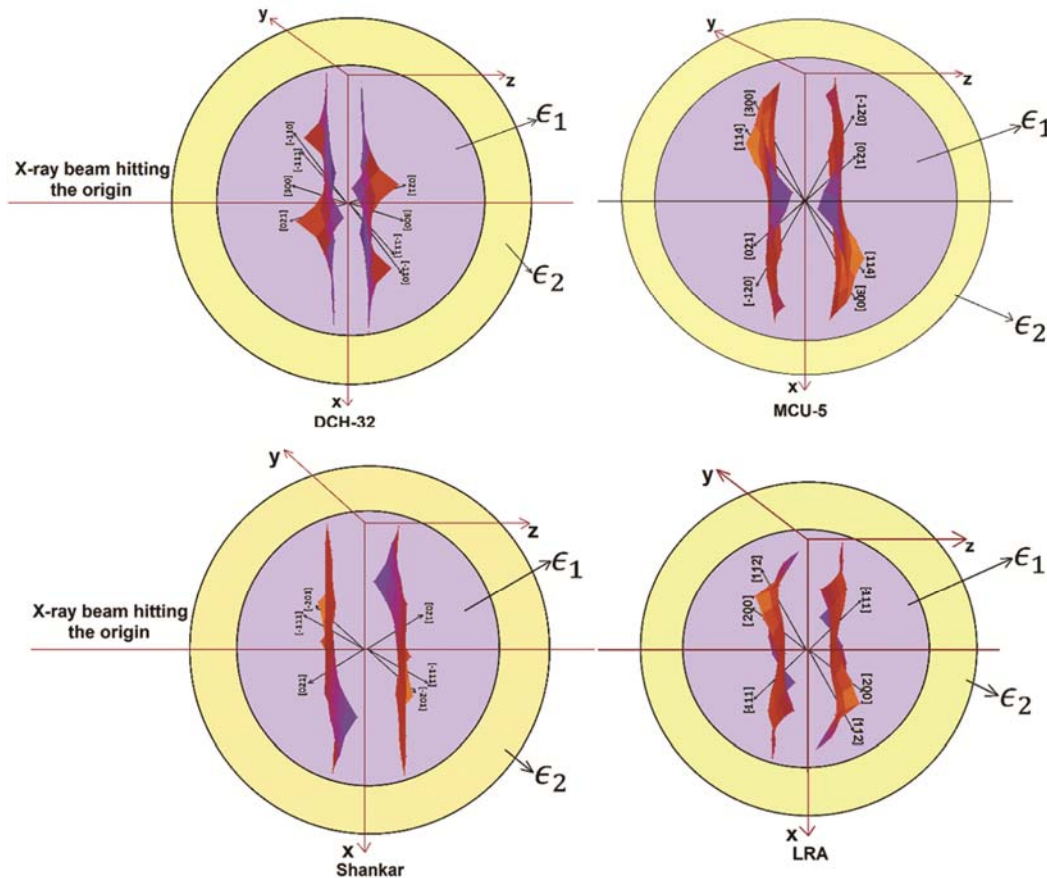


Fig. 7 — Estimated values of epsilon 1 and epsilon 2 for DCH-32, MCU-5, Shankar and LRA

crystallite size and strain among varieties of cotton fibres. From these Eigen values, we have computed mean variation of physical parameters with varieties of cotton fibres.

### 3.3 Dielectric Constant

Lorenz-Mie theory of scattering of electromagnetic radiation by molecules embedded in dielectric spheres has been followed. For small particles, the scattering cross-section decreases to zero for the ratios of core to total radius ( $q = A/B$ ). Expression for polarizability of concentric spheres are given in Rayleigh limit<sup>20</sup>. From this, the dielectric constant of the medium must be intermediate between that of the core and the shell, as shown below:

$$q^3 = \frac{-(\varepsilon_2 - 1)(\varepsilon_1 + 2\varepsilon_2)}{(2\varepsilon_2 + 1)(\varepsilon_1 - \varepsilon_2)} \dots (5)$$

We have used this relation in order to compute the different regions of dielectric constant ( $\varepsilon_1$  and  $\varepsilon_2$ ) responsible for Bragg reflections of varying intensities and widths in the x-ray diffraction pattern from cotton fibres. We have taken crystallite sizes computed for various Bragg reflections after normalization for this purpose. By taking  $b$  in the expression for  $q$  to be that of maximum crystallite size and to be varying for different Bragg reflections, we have chi-square minimized the computed  $q^3$  value of above equation by varying the parameters  $\varepsilon_1$  and  $\varepsilon_2$ . The results are given in Tables 2-5. From this analysis of the crystallite size data of various Bragg reflections observed in cotton fibres, we could compute the average values of  $\varepsilon_1$  as 6.8 and  $\varepsilon_2$  as 0.62, 0.79, 0.76 and 0.77 for DCH-32, MCU-5, Shankar, and LRA cotton fibres respectively. The values are in agreement with reported epsilon value for cellulose which is 6.8. The possible appearance of a material over and above cellulose with a dielectric constant  $\varepsilon_2$  in naturally occurring cotton fibres is shown in Fig. 7 for all the considered cotton fibres.

## 4 Conclusion

4.1 Functional data analysis has given a robust method for extracting the correlation between physical properties and cotton fibre varieties by depicting dependence of physical properties with respect to the microstructural parameters.

4.2 The crystallite shape in each variety of cotton fibres shows a different type of topography.

4.3 Volume of the crystallite region in each of the variety of cotton fibres is estimated as DCH-32 =  $5.65 \times 10^{-25}$  m<sup>3</sup>, MCU-5 =  $4.5 \times 10^{-25}$  m<sup>3</sup>, Shankar =  $4.2 \times 10^{-25}$  m<sup>3</sup> and for LRA =  $2.8 \times 10^{-25}$  m<sup>3</sup>, which shows a variation indicating that the ordered region is different.

4.4 For the first time, using XRD data and employing Lorenz-Mie theory of scattering of electromagnetic radiation by molecules embedded in dielectric spheres, we have computed the dielectric constant of major material cellulose component along with amorphous region with a dielectric constant of 0.74, which explains the variation in scattered intensity along different Bragg angles in addition to the usual condition of Bragg's law.

4.5 This study suggests that DCH-32 cotton fibre has more ordered region than any other variety.

## Acknowledgement

Authors are thankful to the University Grants Commission, New Delhi, India for the funding support to the University of Mysore through UPE and CPEPA major research projects.

## References

- 1 Niranjan A R, Divakara S & Somashekar R, *Indian J Fibre Text Res*, 36 (2011) 10.
- 2 Samir O M & Somashekar R, *Bulletin Materials Science*, 30 (2007) 503.
- 3 Nanda Prakash M B, Thejas urs G, Ananda H T & Somashekar R, *AIP Proceeding*, 1591 (2014) 816.
- 4 Nishiyama Y, Johnson G P & French A D, *Cellulose*, 19(2) (2012) 319.
- 5 Glasser W G, Atalla R H, Blackwell J, Brown R M, Burchard W, French A D & Nishiyama Y, *Cellulose*, 19(3) (2012) 589.
- 6 Chattopadhyay DP & Patel BH, *Natural Fibres*, 8(1)(2011) 39.
- 7 Lin H, Yao L R, Chen Y Y & Wang H, *Fibres Polym*, 9(2) (2008) 113.
- 8 Mohsin M, Carr C M & Rigout M, *Fibres Polym*, 14(5) (2013) 724.
- 9 Zhao P, Liu S, Xiong K, Wang W & Liu Y, *Fibres Polym*, 17(4) (2016) 569.
- 10 Günesolu C, Günesolu S, Wei S & Guo Z, *Fibres Polym*, 17(3)(2016) 402.
- 11 Kamalha E, Kiberu J, Nibikora I, Mwasiagi J I & Omollo E, *Natural Fibres*, (2017) 1.
- 12 Rupashree M P, Thejas Urs G, Mahadeva J, Babu K M & Somashekar R, *Basic Appl Eng Res*, 1(4) (2014) 68.
- 13 Koli G P, Patil D V & Bagade A B, *Int Current Microbiol Appl Sci*, 3(11) (2014) 628.
- 14 Divakara S, Siddaraju G N & Somashekar R, *Fibres Polym*, 11(6) (2010) 861.
- 15 Chen R, Runying, Kathryn A, Jakes & Dennis W Foreman, *Appl Polym Sci*, 93(5) (2004) 2019.

- 16 Muruges B K, Selvadass M, Somashekar R, Niranjana A R & Samir O M, *Int J Carbohydrate Res*, 1(14) (2012)10.
- 17 Thejas Urs G, Sangappa Y, Byrappa K & Somashekar R, *AIP Proceedings*, 1832(1) (2017) 040012.
- 18 Divakara S, Niranjana A R & Somashekar R, *Cellulose*, 16 (6) (2009) 1187.
- 19 Urs Thejas Gopal Krishne, Karthik Bharath, Sangappa Yallappa & Somashekar Rudrappa, *J Appl Crystallography*, 49(2) (2016) 594.
- 20 Kerker Milton, *Aerosol Sci Technol* 1(3) (1982) 275.
- 21 Zhao H, Kwak J H, Zhang Z C, Brown H M, Arey B W & Holladay J E, *Carbohydrate Poly*, 68(2) (2007) 235.